# Characterizing the Molecular Dimensions of Flexible Dendrimers in Solution

Janine L. Thoma,[1] Stuart A. McNelles,[2] Alex Adronov*,[2] Jean Duhamel*,[1]

Institute for Polymer Research, Waterloo Institute for Nanotechnology, Department of Chemistry, University of Waterloo, ON N2L 3G1, Canada

Department of Chemistry and the Brockhouse Institute for Materials Research, McMaster University, 1280 Main Street West, Hamilton ON L8S 4L8, Canada

**Introduction**

The molecular dimensions of rigid macromolecules in solution are customarily determined by using fluorescence resonance energy transfer or FRET. FRET requires that one donor and one acceptor chromophore pair be covalently attached at two specific sites of a rigid macromolecule, traditionally the end groups. The end-to-end distance of such a macromolecule can then be calculated from the FRET efficiency if the Förster radius for the energy donor and acceptor is known. However, the mathematical complexity involved in the determination of the distance between the donor and acceptor increases greatly when the macromolecule is flexible. The FRET efficiency observed for such a construct would change as a function of time with FRET being more likely when the donor and acceptor are closer to each other. The mathematical handling of a time-dependent FRET efficiency is usually more challenging. Even more complex are those flexible macromolecules which have more than two ends or can be randomly labeled. In this case, both end-to-end distribution and backbone dynamics are unknown. Dendrimers are a case in point since they are flexible macromolecules with more than two terminals.

Another technique available to study the dynamics of macromolecules in solution is pyrene excimer formation/fluorescence (PEF). Pyrene excimer formation occurs upon physical encounter between an excited and a ground-state pyrene molecule. Thus contrary to FRET, for which the rate constant of FRET depends on the sixth power of the distance separating the donor from the acceptor, the rate constant of PEF depends solely on the local pyrene concentration in the pyrene-labeled macromolecule. Both the pyrene monomer and excimer emission can be characterized using either Steady-State (SSF) or Time-Resolved (TRF) fluorescence. From SSF measurements, the intensity of the monomer and excimer can be quantified by looking at the fluorescence intensity ratio of excimer to monomer, namely the $I_E/I_M$ ratio. TRF measurements yield both the pyrene monomer and excimer decay which can be fitted with the Model Free Analysis (MFA).[1] The MFA allows the identification of the molar fractions of different pyrene species present in the macromolecule such as $f_{free}$, $f_{diff}$, and $f_{agg}$ which represent those pyrene labels that do not form excimer and emit as if they were free in solution ($Py_{free}^*$), form excimer upon diffusive encounters ($Py_{diff}^*$), and form excimer instantaneously upon direct excitation of a pyrene aggregate ($Py_{agg}^*$). The MFA also yields the average rate constant of excimer formation, $\langle k \rangle$. The average rate constant of excimer formation is directly related to the local concentration of pyrene, $[Py]_{loc}$, as shown in Equation 1.

$$\langle k \rangle = k_{diff} \times [Py]_{loc} \qquad (1)$$

In Equation 1, $\langle k \rangle$, $k_{diff}$, and $[Py]_{loc}$ are the average rate constant of excimer formation, the rate constant of excimer formation via diffusive processes, and the local concentration of pyrene in the macromolecule, respectively. $[Py]_{loc}$ is equal to the ratio of the number of moles of pyrene divided by the macromolecular volume.

Dendrimers are branched macromolecules which possess precise architectures containing multiple reactive terminals. As a result, their use in the encapsulation of metal nanoparticles as well as drug carriers has been well studied.[2,3] They are typically grown in generations, however the preparation of high generation dendrimers is challenging due to the crowding of the functional terminals as suggested by De Gennes.[4] The characterization of the dimensions and dynamics of these branched macromolecules can be achieved by labeling a dendrimer with a pyrene derivative, as shown in Figure 1, and then applying the MFA to isolate each of the different pyrene species, calculate $\langle k \rangle$, and investigate the relationship between $\langle k \rangle$ and $[Py]_{loc}$ for a series of dendrimers.

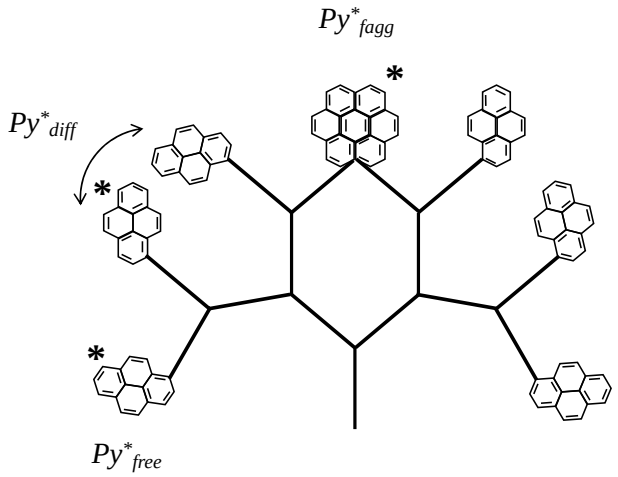


**Figure 1.** Schematic representation of each of the pyrene species identified by the MFA of fluorescence decays acquired for pyrene-labeled dendrimers.

**Results and Discussion**

A series of well-defined dendrimers with a bis(hydroxymethyl)propionic acid backbone were synthesized. Six generations containing 2, 4, 8, 16, 32, and 64 terminals were reacted with 1-pyrenebutyric acid to prepare pyrene labeled dendrimers (PyLDs) ($Py_x$-G(N) where $x$ is the number of pyrenyl groups, $2^N$, and $N$ is the generation number, 1-6). Two other dendrimers were synthesized using 'click' chemistry resulting in a larger spacer between the terminal pyrene labels and the focal point of the dendrimer ($Py_{64}$-G6-spacer) with one of the two constructs also containing a pyrene at the focal point of the dendrimer ($Py_{64+1}$-G6-spacer). Since one pyrene group becomes excited and absorbs a photon of light, the number of ground-state pyrenes in an $N$-generation dendrimer equals $2^N$-1. If the volume of the dendrimer can be approximated to that of a sphere, the local concentration of pyrene in a dendrimer is given by Equation 2.

(2)

In Equation 2, $r$ is the radius of the dendrimer. In turn, $r$ can be equated to the square root of the average squared end-to-end distance, $<L_{Py}^2>^{1/2}$, of the dendrimer as shown in Equation 3.

$$r = <L_{Py}^2>^{0.5}/2 \quad (3)$$

To determine $<L_{Py}^2>^{1/2}$, all $Py_x$-G(N) dendrimers could be broken down into segments containing 'a' and 'b' atoms for the linker connecting pyrene to the first branch point and each segment spanning two branch points. The bond length was approximated by $l$. The expressions for $<L_{Py}^2>^{1/2}$ obtained for all $Py_x$-G(N) constructs are listed in Equations 4 - 6.

$$< L_{Py}^2 >= l^2\left(1+2a+b\frac{N\times 2^N-2^{N+1}+2}{2^N-1}\right) \quad (4)$$

For $Py_{64}$-G6-Spacer:
$$< L_{Py}^2 >= l^2\left(1+2a+b\frac{258}{63}+c\frac{112}{63}\right) \quad (5)$$

For $Py_{64+1}$-G6-Spacer:
$$< L_{Py}^2 >= l^2\left(1+2a+b\frac{258}{64}+c\frac{112}{64}+\frac{(a+2.5b+c+d)}{64}\right) \quad (6)$$

Once $<L_{Py}^2>^{1/2}$ was calculated for each pyrene-labeled dendron (PyLD), it could be applied to determine the radius of the dendrimer in Equation 3, which was then introduced into Equation 2 to determine $[Py]_{loc}$. The relationship between $<k>$ determined experimentally from the MFA of fluorescence decays and the calculated expression of

$[Py]_{loc}$ was expected to be linear according to Equation 1. In Figure 2A, $\langle k \rangle$ was plotted as a function of $[Py]_{loc}$ for each dendrimer and it was found to increase linearly for $Py_2$-G1 to $Py_{32}$-G5 but the $\langle k \rangle$ value for $Py_{64}$-G6 fell below its expected value. This discrepancy was attributed to pyrene aggregation as illustrated in Figure 2B where $f_{agg}$ was plotted as a function of generation number. For G1 to G4, the fraction of aggregated pyrenes remained below 0.05 but it increased for G5 and G6 as the number of terminal ends increased to 32 and 64.

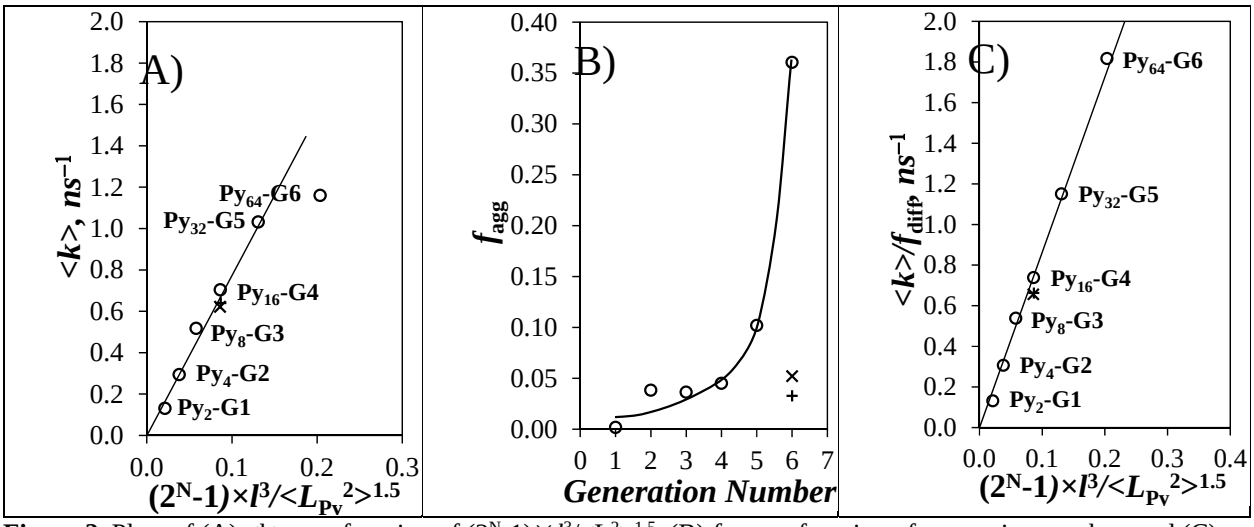


**Figure 2.** Plots of (A) <k> as a function of $(2^N\text{-}1) \times l^3/\langle L^2 \rangle^{1.5}$, (B) $f_{agg}$ as a function of generation number, and (C) $\langle k \rangle / f_{diff}$ as a function of $(2^N\text{-}1) \times l^3/\langle L^2 \rangle^{1.5}$ for the PyLDs in degassed THF. (○) $Py_x$-G(N), (×) $Py_{64}$-G6-spacer, (+)$Py_{64+1}$-G6-spacer.

According to Equation 1, $\langle k \rangle$ is proportional to $[Py]_{loc}$ which assumes that all pyrene labels are non-aggregated. However G6 showed substantial pyrene aggregation which reduced $[Py]_{loc}$ and explained why $\langle k \rangle$ fell below the line of best fit in Figure 2A. To account for the reduction in non-aggregated ground-state pyrene labels, $\langle k \rangle / f_{diff}$ was plotted in lieu of $\langle k \rangle$ as a function of $N$ in Figure 2C resulting in a perfectly straight line.

In conclusion, $\langle k \rangle$ was found to be proportional to $(2^N\text{–}1)/\langle L_{Py}^2 \rangle^{1/2}$ for 8 PyLDs. Assuming an $l$ value of 1.25 Å in Equations 4-6, the dimension of the PyLDs was found to range between 4.5 and 8.5 Å. The two PyLDs with a spacer, namely $Py_{64}$-G6-spacer and $Py_{64+1}$-G6-spacer, had $\langle L_{Py}^2 \rangle^{1/2}$ values equal to 11.3 Å and 11.2 Å, respectively. The determination of the dimension, dynamics, and level of terminal aggregation of the PyLDs by PEF will allow researchers to better understand the behavior of dendrimers in solution for uses as drug or metal nanoparticle carriers.

**References**

(1) Duhamel, J. New Insights in the Study of Pyrene Excimer Fluorescence to Characterize Macromolecules and their supramolecular Assemblies in Solution. *Langmuir* **2012**, 28, 6527- 6538.
(2) Sharma, A. K.; Gothwal, A.; Kesharwani, P.; Alsaab, H.; Iyer, A.K.; Gupta, U. Dendrimer Nanoarchitectures for Cancer Diagnosis and Anticancer Drug Delivery. *Drug Discov. Today* **2017**, *22*, 314-326.
(3) Crooks, R. M.; Zhao, M.; Sun, L.; Chechik, V.; Yeung, L. K. Dendrimer-Encapsulated Metal Nanoparticles: Synthesis, Characterization, and Applications to Catalysis. *Acc. Chem. Res.* **2001**, 34, 181-190.
(4) De Gennes, P. G.; Hervet, H. Statistics of Starburst Polymers. *J. Phys. Lett.* **1983**, 44, 351-360.